

# Effect of Nano Domains in the Hole Mobility of MEH-PPV

## Beamline

17A X-ray Powder Diffraction beamline

17B X-ray Scattering beamline

## Authors

A. R. Inigo, Y. F. Huang and W.S. Fann

Academia Sinica & National Taiwan University, Taipei, Taiwan

U. Jeng, C. H. Hsu, H. S. Sheu and H. Y. Lee

National Synchrotron Radiation Research Center, Hsinchu, Taiwan

A. C. Su

National Sun Yat-sen University, Kaohsiung, Taiwan

K. Y. Peng and S. A. Chen

National Tsing Hua University, Hsinchu, Taiwan

*The influence of nano domains in a model organic semiconductor, MEH-PPV has been analyzed by different processing conditions. It was observed that not the presence of the domains which affects the charge transport, but the degree of orientation of the domains which influences the charge carrier mobility. Further, it is shown that the homogeneous medium is preferred for better charge transport, where the charge carrier seems smoother pathways for hopping.*

Charge carrier mobility in optoelectronic devices based on organic electronic materials, is directly related to the order/disorder present in the material, and currently limits many potential applications. Methods capable of improving polymer morphology and hence mobility are thus of considerable interest not only scientifically but also technologically. The development of ordered crystal-like films, of up to macroscopic size, has been successful in improving charge transport characteristics (i.e. mobility) in poly(thiophene) derivatives. The large mobility increase recently obtained in ladder type polymers (i.e. from  $4 \times 10^{-6} \text{ cm}^2/\text{Vs}$  to  $0.1 \text{ cm}^2/\text{Vs}$  in poly(benzobizimidobenzophenonethroline) (BBL)) is at least partly the result of morphological changes which provided greater intermolecular order (as proved by atomic force microscopy and X-ray diffraction). One of the most studied of these PPV derivative polymers is MEH-PPV. A soluble derivative of PPV, it has a variety of conformations depending upon its intrinsic chemical properties and processing conditions. Much research has focused on understanding the relationships between morphology and luminescent properties. Morphology variation can lead to different kinds of charge carrier transport ranging from highly dispersive to non-dispersive. Using different solvents (i.e. toluene (TL) and chlorobenzene (CB)), we demonstrated that TL-cast MEH-PPV films have a larger order-like domain size but fewer domains than CB-cast MEH-PPV films. The mobility in TL-cast films was higher than that of CB-cast films. These results suggest that mobility might be further

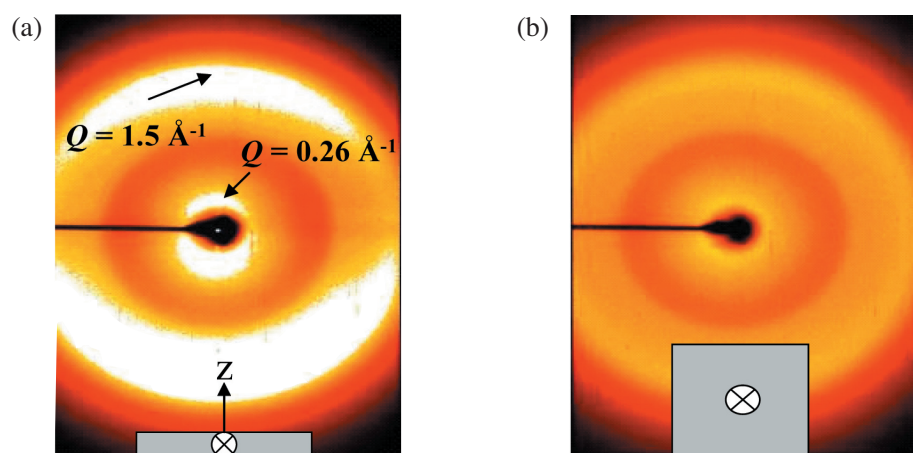


Fig. 1: Grazing-incidence WAXS data collected in the (a) depth and (b) in-plane directions, respectively.

enhanced by reducing the density of nano-domains in polymer films.

In this work, thin films were prepared by drop-casting method from 5mg/cc of MEH-PPV in chlorobenzene (CB) on ITO-coated substrates. During the deposition process, in one group of films, an electric field ( $E_{\text{cast}}$ ) was applied parallel to the substrate in order to inhibit domain formation (these are henceforth denoted “E-field cast”). A second group of films (henceforth denoted “as-cast”) served as a control group in which no electric field was applied during deposition. In third group, the as-cast films were annealed at 215 °C for about 12 hours. In order to understand the reasons for the variation in mobility, we investigated the underlying morphological differences by wide angle X-ray scattering (WAXS).

**As-cast films:** The GI-WAXS patterns showed no sharp diffraction peaks; only halos are observed in both the in-plane and depth directions of the film (Fig. 1), indicating general absence of large domains of three-dimensional (3D) positional order in the film. It is nevertheless convenient to interpret the diffraction pattern in terms of the concept of nanocrystalline domains, which has been adopted to interpret medium-range order (MRO) in materials such as “amorphous” silicon that lie somewhat beyond the borderline of traditional definition of crystals. From the widths of the halos, the size of chain-packed MEH-PPV nanocrystalline domain is estimated as ca. 20 Å for both the  $Q = 1.01$  and  $1.48 \text{ \AA}^{-1}$  halos (which correspond to d-spacing values of 6.3 and 4.3 Å, respectively), and 100 Å for the  $0.26 \text{ \AA}^{-1}$  halo (which corresponds to 24 Å in d-spacing). The positional order does not extend beyond ca. 4 d-spacing values and is indeed medium-range at most.

Scattering profiles along the depth and the in-plane directions are similar in shape, but much stronger in intensity for the former case. This suggests structural anisotropy along the film normal. To quantitatively compare the scattering intensities in the two directions, we further correct the WAXS data for sample transmission and beam path length, as detailed in Appendix. The asymmetrical scattering pattern, emphasized in the depth direction, is better illustrated by the 2D scattering image taken from the free-standing film at quasi-parallel incidence. In contrast, the corresponding normal-incidence WAXS pattern (Fig. 1) exhibits Debye-Scherrer cone-like features of circular symmetry, indicating that there is no preference in the in-plane orientation.

The observations of nanometer-sized domains and in-plane isotropy are consistent with previous PLM, TEM, and WAXS results of high beam-incidence angles, which had led to the conclusion that the as-cast films are largely isotropic and disordered in the in-plane direction. It was previously indicated a similar asymmetry structure in the depth direction from their 2D WAXS pattern of near-parallel incidence over a *stretched* MEH-PPV film cast from tetrahydrofuran. This uniaxial structural anisotropy, also identified for the MEH-PPV film cast from chlorobenzene, is therefore very likely a general feature qualitatively shared among as-cast films. Nevertheless, there may exist delicate differences in quantitative aspects of nanodomain development and roughness of the nanodomain/matrix interface under different processing conditions.

**Anisotropy:** There is one more point to be made on the basis of Fig. 1(b): the much higher intensity at  $Q = 0.26 \text{ \AA}^{-1}$  in the depth direction, compared to that in the in-plane direction, indicates that the bilayers within the MRO nanodomains prefer to stack along film normal. From the  $0.26 \text{ \AA}^{-1}$  peak intensities, we extract an orientation parameter  $p = (I_d - I_i)/(I_d + I_i) = \text{ca. } 0.6$ , where  $I_d$  and  $I_i$  represent peak intensities in the depth and the in-plane directions, respectively. This preferred bilayer stacking along the film normal is attributed to the preference of alkyl side chains towards the air-liquid interface (thereby reducing surface tension), which serves to “guide” (via “amphophilic” nature of MEH-PPV, in which incompatibility exists between the aromatic backbone and the covalently attached alkyl side-chains) the alignment of subsequently assembled domains upon gradual depletion of solvent through diffusion and evaporation along the film normal.

In the present as-cast MEH-PPV film, the scattering arc centered around  $Q = 0.26 \text{ \AA}^{-1}$  in the vertical direction (Fig. 1(a)) signifies this uniaxial orientation, with the spread angle of the arc reflecting a non-perfect alignment of the MEH-PPV nanodomains in the surface normal direction. It is therefore indeed plausible that this tendency of preferred orientation, observed via diffraction or spectroscopic evidences for different conjugated polymers grafted with alkyl side chains, is likely a general phenomenon attributable to the consistent presence of alkyl side chains in these polymers. Complementary evidences from surface spectroscopy would be preferable but this is beyond the scope of present work.

**Annealed films:** Structural features observed above for the as-cast MEH-PPV films, bearing solvent-induced characteristics that are kinetically trapped during film formation, are inherently metastable. This is most clearly demonstrated by annealing at 210°C. In Fig. 2(a) (inset), the WAXS image taken under a grazing incident beam for the annealed freestanding film of MEH-PPV, demonstrates the dramatic effect of annealing on the film structure. The layering features composed of two overlapping arcs in the depth direction of the as-cast film (Fig. 1(a)) converge into a single spacing of 17.5 Å (at  $Q = 0.36 \pm 0.02 \text{ \AA}^{-1}$ ) and spread into a circle for this case of annealed film. Correspondingly, the normal-incidence WAXS pattern (cf. Fig. 2(b)) shows Debye-Scherrer ring at the same  $Q = 0.36 \text{ \AA}^{-1}$  position. Clearly, the structure of the MEH-PPV film becomes more isotropic upon annealing. In addition, the transient bilayer packing (24.2 Å in spacing) in the as-cast film transforms into its thermodynamically favored counterpart (17.5 ± 1.0 Å in spacing) during annealing.

From the widths of the  $0.36 \text{ \AA}^{-1}$  peaks fitted using Lorentzian profiles (solid curves in Fig. 6(a) and (b)), we estimate that the coherent length of the bilayers amounts to ca. 125 and 110 Å in the depth and the in-plane directions, respectively. These are comparable to that (ca. 100 Å) obtained for the as-cast film. It therefore follows that annealing at 210°C serves mainly to randomize the kinetically oriented nanodomains in the film with insignificant changes in the domain size, although minor adjustment of the MRO within nanodomains indeed results in a converged layer spacing of 17.5 Å. The randomized reorientation of nanodomains in the annealed film may also be perceived by the relative intensity changes in the two peaks at  $Q = 0.36 \text{ \AA}^{-1}$  (bilayer spacing along the  $b$ -axis) and  $1.5 \text{ \AA}^{-1}$  (inter-backbone distance along  $a$ -axis) (Fig. 1 and Fig. 2). Similar structural characteristics for toluene-cast MEH-PPV films annealed briefly (5 min) at 230°C were observed by selected-area electron diffraction in a recently study by Chen et al.<sup>15</sup> Although not given here, we have also made similar studies on MEH-PPV films cast from chlorobenzene: the general feature of anisotropy along depth direction persists in the as-cast film, with only minor differences in structural details. Annealing of the chlorobenzene-cast film at 210°C results in essentially the same structure as that presented here for the toluene-cast annealed film.

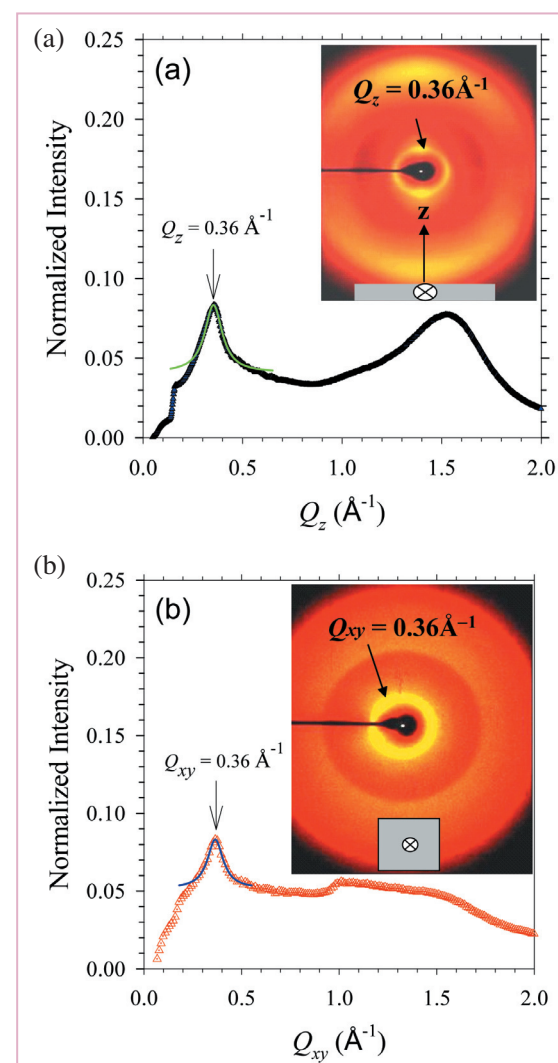


**Fig. 2:** Grazing-incidence WAXS profile in the (a) depth (b) in-plane directions.

It is therefore concluded that, aside from minor structural reorganization within the nanodomains towards the thermodynamically favored bilayer packing with lamellar spacing of 17.5 Å, the main effect of heat treatment at an elevated temperature is the disruption of orientation of nanodomains during film formation upon solvent evaporation. Both the rotation of side chains for shorter bilayer spacing and the reorientation of the ordered domains for a more isotropic structure, proposed here for the structural changes of the MEH-PPV film upon isothermal annealing, are consistent with the DSC results of Chen et al., in which the transformation was shown thermally weak.

**E-cast films:** The WAXS data measured both in the in-plane and depth directions of the films exhibit no sharp scattering peaks, indicating a lack of crystalline structure. Nevertheless, the substantial halos

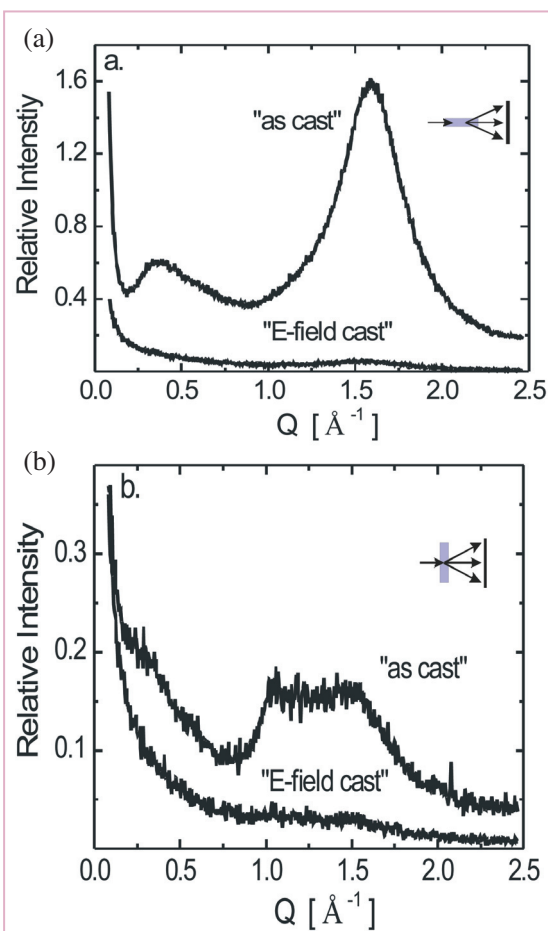


**Fig. 3:** WAXS data for “as-cast” and “E-field cast” films of MEH-PPV as measured in the (a) normal-to-plane (depth) direction (charge carrier transport direction) and (b) in-plane direction.

observed for the “as-cast” film in both directions indicates the existence of ordered domains in largely random polymer network. This ordering gives rise to the local density fluctuations that provide scattering contrast. In the charge carrier transport direction, the “as-cast” film shows broadened amorphous halos peaked at  $Q = 0.37$  and  $1.59\text{\AA}^{-1}$ . The corresponding Bragg-like characteristic-d-spacing ( $d = 2\pi/Q$ ) obtained from the peak positions are  $17.0\text{\AA}$  and  $4.1\text{\AA}$ . The domain sizes ( $D$ ) estimated from the full width at half maximum ( $\Delta Q$ ) of the scattering peaks using  $D = 2\pi/\Delta Q$  is  $\sim 80\text{\AA}$  and  $\sim 16\text{\AA}$  respectively. The characteristic spacing  $4.1\text{\AA}$  corresponds to the benzene ring packing distance between neighboring polymers, whereas the characteristic spacing of  $17\text{\AA}$  corresponds to a possible bilayer structure of MEH-PPV. In the in-plane direction, the WAXS result for the as cast film shows an additional characteristic length of  $6.3\text{\AA}$  at  $Q = 1.0\text{\AA}^{-1}$ . This is assigned to the characteristic length of the monomeric repeat along the backbone of MEH-PPV.

From X-Ray reflectivity and density measurements, the volume fraction of the ordered domains is estimated as  $0.52 \pm 0.13$ ; however, a complete analysis of the “as-cast” and annealed are discussed in the following. In contrast, the featureless WAXS (Fig. 2(a) and 2(b)) for the “E-field cast” film in both in-plane and depth directions imply a completely amorphous structure with no short-range ordered domains. Clearly, inhomogeneity is reduced by the applied E-field during film formation. Likely, the interaction between the E-field and polar parts of MEH-PPV prevents any kind of ordered packing during the solvent drying process. In other words, the interactions between the applied E-field and the polar parts of MEH-PPV are stronger than the Van der Waal interactions between individual MEHPPV polymers that lead to packing.

In summary, the domains seem to affect the charge carrier transport. The presence of domains itself is not only important but the orientation of the domains are more important. In addition to this, destruction of these domains increases the drift mobility by providing smoother hopping of charge carriers.

## Experimental Station

### X-ray Scattering end station

### Publications

- U.-S. Jeng, *et al.*, Macromolecules **38**, 6566, (2005).
- A. R. Inigo, *et al.*, Advanced Materials **17**, 1835 (2005).
- A. R. Inigo, *et al.*, Physical Review B. **69**, 075201 (2004).
- C. H. Tan, *et al.*, Organic Electronics **3**, 85 (2002).

### Contact E-mail

fann@gate.sinica.edu.tw